PHYSICAL REVIEW B **90**, 201112(R) (2014)

Surface control of flexoelectricity

Massimiliano Stengel
ICREA - Institució Catalana de Recerca i Estudis Avançats, 08010 Barcelona, Spain
and Institut de Ciència de Materials de Barcelona (ICMAB-CSIC), Campus UAB, 08193 Bellaterra, Spain
(Received 13 February 2014; revised manuscript received 29 October 2014; published 24 November 2014)

The polarization response of a material to a strain gradient, known as flexoelectricity, holds great promise for novel electromechanical applications. Despite considerable recent progress, however, the effect remains poorly understood. From both the fundamental and practical viewpoints, it is of crucial importance to know whether the coupling coefficients are primarily governed by the properties of the bulk material or by the details of the sample surface. Here we provide, by means of first-principles calculations, quantitative evidence supporting the latter scenario. In particular, we demonstrate that a $SrTiO_3$ film can yield a positive or negative voltage upon bending, depending on whether it is terminated by a TiO_2 or SrO layer. This result points to a full control of the flexoelectric effect via surface/interface engineering, opening exciting new avenues for device design.

DOI: 10.1103/PhysRevB.90.201112 PACS number(s): 71.15.−m, 77.65.−j

Flexoelectricity is a universal property of all insulators, whereby a macroscopic electrical polarization is generated in response to an inhomogeneous mechanical strain [1]. The recent surge of interest in this phenomenon [2] has come with the realization that strain gradients can be huge at the nanoscale, and generate a large enough polarization to rival conventional piezoelectricity [3]. Long regarded as a drawback in the operation of thin-film devices (e.g., ferroelectric memories [4], or light-emitting diodes in foldable electronics [5]), strain gradients are now being increasingly recognized as a rich playground for exploring new, potentially useful, functionalities [6,7]. Future progress towards practical applications crucially relies on identifying the microscopic mechanisms that are most effective at delivering a large electrical response, and on harnessing them via specific materials-design rules. Unfortunately, such a fundamental knowledge is currently very limited.

A central (yet vastly unexplored) question concerns the role played by the sample surfaces. Both simplified physical models [8] and quantum-mechanical theory [9,10] predict their contribution to be nonnegligible in the thermodynamic limit. This fact, in principle, calls for a substantial revision of the currently established device design strategies, where only bulk electromechanical properties (such as piezoelectricity [11] and/or electrostriction) are typically taken into account [12]. In practice, however, there are currently little indications on the importance of the aforementioned surface effects (only order-of-magnitude estimates are available [8], which predict their contribution to be comparable to bulk effects), nor on their microscopic physical nature, so the necessity for their explicit inclusion in the models remains open to debate. It appears unlikely that such indications will emerge from the experiments alone, at least in the near future: as the bulk and surface contributions scale identically with sample size (unlike other interface-related phenomena in oxides, e.g., the dielectric "dead" layer [13,14]), they appear difficult or impossible to disentangle by purely electrical means. In this context, theoretical modeling, especially by means of first-principles electronic-structure methods, can be of great help.

Building on the work of Martin [11] and Resta [15], Hong and Vanderbilt [9,16] have recently devised a promising route to addressing the flexoelectric problem at a fundamental quantum-mechanical level, and applied it to calculating the response properties of a number of bulk materials in the framework of density-functional theory (DFT). However, even at the bulk level, a complete determination of the full flexoelectric tensor has not been achieved yet, as the electronic contribution to the transversal components is still missing [16]. Furthermore, the impact of surface effects was not considered in Refs. [9,16], nor in any other first-principles study [17,18] reported to date. Very recent advances promoted by the author [10,19] have now opened the way to filling both gaps, by combining density-functional perturbation theory (DFPT)—-the linear-response version of DFT—with a covariant formulation of electrostatics in the coordinate system of the deformed body. Here we use such a methodology to study the flexoelectric response of $SrTiO_3$, one of the most important flexoelectric materials, and the best known experimentally [20]. Our results, in addition to providing a complete physical picture of the effect, demonstrate that the surface indeed matters: by modifying the atomically thin termination layer, one can tune, and even reverse, the voltage response of a macroscopically thick film.

The flexoelectric performance of an insulating material can be conveniently quantified as the open-circuit voltage, ΔV, that is linearly induced by a strain-gradient deformation [see Fig. 1(c)] in the limit of a large film thickness, t,

$$\varphi_{x\lambda,\beta\gamma} = \lim_{t\to\infty} \frac{1}{t} \frac{\partial \Delta V}{\partial \varepsilon_{\beta\gamma,\lambda}}. \tag{1}$$

Here $\varepsilon_{\beta\gamma,\lambda} = \partial\varepsilon_{\beta\gamma}/\partial r_\lambda$ is the gradient of the symmetric strain tensor ($\varepsilon_{\beta\gamma}$) along the Cartesian direction r_λ, and x indicates the direction normal to the surface; the relevant components of $\varepsilon_{\beta\gamma,\lambda}$ in the context of this work are illustrated in Figs. 1(d)–1(f). Remarkably, although $\varphi_{x\lambda,\beta\gamma}$ (referred to as "flexovoltage" coefficients henceforth) is a macroscopic response property of the system, it is known [10] to contain *both* bulk- and surface-specific contributions,

$$\varphi_{x\lambda,\beta\gamma} = \varphi^{\rm bulk}_{x\lambda,\beta\gamma} + \varphi^{\rm surf}_{x\lambda,\beta\gamma}. \tag{2}$$

The former term is given by $\varphi^{\rm bulk}_{x\lambda,\beta\gamma} = \mu^{\rm bulk}_{x\lambda,\beta\gamma}/(\epsilon_0\epsilon_{xx})$, where $\boldsymbol{\mu}^{\rm bulk}$ is the bulk flexoelectric tensor, $\boldsymbol{\epsilon}$ is the macroscopic dielectric tensor, and ϵ_0 is the vacuum permittivity. The latter term, $\varphi^{\rm surf}_{x\lambda,\beta\gamma}$, originates from surface piezoelectric

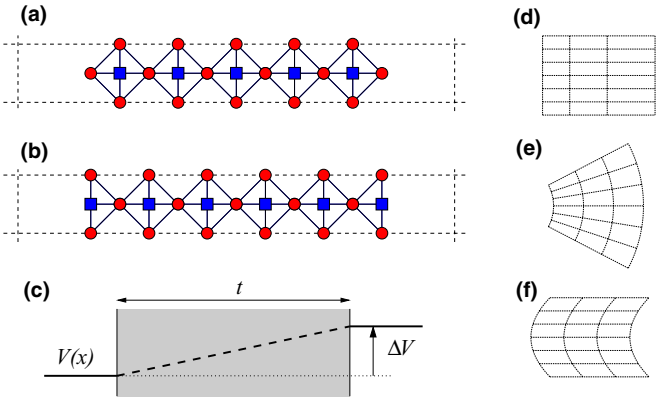

FIG. 1. (Color online) Schematic illustration of the computational setup. Panels (a) and (b) show the supercell models of the SrO- (a) and TiO_2-terminated (b) $SrTiO_3$ slabs (Ti and O atoms are represented as squares and circles; Sr atoms are not shown). Panel (c) shows the induced open-circuit voltage, ΔV, induced by a longitudinal [$\varepsilon_{xx,x}$, (d)], transversal [$\varepsilon_{yy,x}$, (e)]. or shear [$\varepsilon_{xy,y}$, (f)] strain-gradient deformation.

effects [8,10,21], which are present in any material regardless of crystal symmetry. Based on the total flexovoltage coefficient of Eq. (2), the short-circuit flexoelectric response of an electroded slab is then readily given by

$$\mu_{x\lambda,\beta\gamma} = \epsilon_0 \epsilon_{xx} \left(\varphi_{x\lambda,\beta\gamma} + \varphi^{\mathrm{WF}}_{x\lambda,\beta\gamma} \right), \tag{3}$$

where φ^{WF} describes a possible additional contribution coming from the work function of the metal electrodes. (Note that the scaling of the surface contribution to μ with the static *bulk* permittivity is consistent with earlier predictions [22].)

While techniques for calculating both φ^{bulk} and φ^{surf} in a first-principles context have recently been proposed [10,16,19], the determination of the bulk flexoelectric tensor remains challenging, particularly concerning the purely electronic contributions. In fact, directly calculating the bulk polarization response to a strain gradient would require access to the microscopic current density [16,19] induced by a deformation, whose code implementation is not available yet. To overcome this methodological obstacle (and solve for the missing transversal components of φ^{bulk}) we shall compute, rather than the polarization response of the *bulk*, the internal electric field response of a *slab*. The advantage of the latter approach is that it can be carried out with the sole knowledge of the first-order charge density [19]. For the sake of computational convenience, we shall initially focus on "frozen-ion" (in the sense specified in Ref. [10]) deformation of "truncated-bulk" slabs, i.e., with the unperturbed atoms placed at their ideal lattice sites. The impact of full ionic relaxation, which is essential for a quantitative analysis of the flexoelectric effect, is uncomplicated to calculate once the electronic contributions to the bulk tensor are known, and will be dealt with in a later part of this work.

We consider the supercell models illustrated in Figs. 1(a) and 1(b) (i.e., periodically repeated sequences of symmetrically terminated $SrTiO_3$ slabs and vacuum layers), and proceed as follows. First, we calculate how the microscopic charge density of the supercell, $\rho(\mathbf{r})$, responds to a selected set of long-wavelength acoustic phonons, by using DFPT as implemented in the ABINIT [23,24] package. Next, we perform a Taylor expansion (in the wave vector $\mathbf{q}$) of such density response functions, along the lines described in Refs. [10,19]. This analysis readily yields the response to a macroscopic strain gradient in the curvilinear coordinate system of the deformed crystal lattice [10]; in particular, one has

$$\frac{\partial \rho(\mathbf{r})}{\partial \varepsilon_{\beta\gamma,\lambda}} = r_\lambda \rho^{\mathrm{U}}_{\beta\gamma}(\mathbf{r}) + \rho^{\mathrm{G}}_{\lambda,\beta\gamma}(\mathbf{r}), \tag{4}$$

where $\rho^{\mathrm{U,G}}$ are cell-periodic functions [$\rho^{\mathrm{U}} = \partial\rho(\mathbf{r})/\partial\varepsilon_{\beta\gamma}$ describes the response to a uniform strain, while ρ^{G} is the additional contribution that is due to the gradient]. Finally, we use ρ^{U} and ρ^{G} to calculate the induced electric field. In the curvilinear frame, the first-order $\mathbf{E}$ is related to the first-order ρ via the modified Gauss's law described in Ref. [10]. (See Supplemental Material [28], note 1, for further details.) As the electric field is related to the potential by $\mathbf{E}(\mathbf{r}) = -\nabla V(\mathbf{r})$, knowledge of the former [and of its first-order variation, $\partial\mathbf{E}(\mathbf{r})/\partial\varepsilon_{\beta\gamma,\lambda}$] then yields the linear variation of the latter, $\partial V(\mathbf{r})/\partial\varepsilon_{\beta\gamma,\lambda}$, and ultimately the sought-after values of the flexovoltage coefficients, φ.

In practice, it is convenient to work with the "macroscopic averages" [25,26] of the $\mathbf{E}$ and ρ response functions, where the oscillations that occur on the scale of the interatomic spacings have been appropriately filtered out. This procedure has two advantages: first, it allows one to identify the relevant electrical properties of the system in a macroscopic context (e.g., internal fields, surface potential offsets, etc.); second, it facilitates the implementation of the Poisson solver by making the problem one-dimensional. In particular, in close analogy to Eq. (4), one can write the normal (x) component of the macroscopically averaged $\mathbf{E}$-field response as

$$\frac{\partial E_x(x)}{\partial \varepsilon_{\beta\beta,x}} = x E^{\mathrm{U}}_{x,\beta\beta}(x) + E^{\mathrm{G}}_{xx,\beta\beta}(x), \tag{5}$$

$$\frac{\partial E_x(x)}{\partial \varepsilon_{xy,y}} = E^{\mathrm{G}}_{xy,xy}(x), \tag{6}$$

where Eq. (5) refers to either the longitudinal or transversal case ($\beta = x,y$), and Eq. (6) concerns a shear deformation. Note that the parallel (y) components of the induced $\mathbf{E}$ field vanish, hence the exclusive focus on E_x. Note also the absence of the uniform-strain contribution in Eq. (6): $E^{\mathrm{U}}_{x,xy}(x)$ vanishes identically in a centrosymmetric slab.

In Figs. 2(a)–2(d) we plot the calculated $E^{\mathrm{U,G}}_x(x)$, corresponding to either a SrO- or a TiO_2-terminated slab and to each of the three types of strain gradients shown in Figs. 1(d)–1(f). (We refer the reader to the Supplemental Material [28], note 1, for the details of the computational methodology and parameters.) As anticipated in Eqs. (5) and (6), there is an important qualitative difference between the longitudinal or transversal response, where the strain gradient is oriented along the surface normal, and the shear response, where it is directed in plane.

In the former two cases, $E^{\mathrm{U}}_{x,\beta\beta}(x)$ (describing the $\mathbf{E}$-field response to a *uniform* strain) is roughly uniform and negative (the oscillations are irrelevant on a macroscopic scale) in a thin region surrounding the surface layer. This is consistent with the expected behavior of the electrostatic potential upon

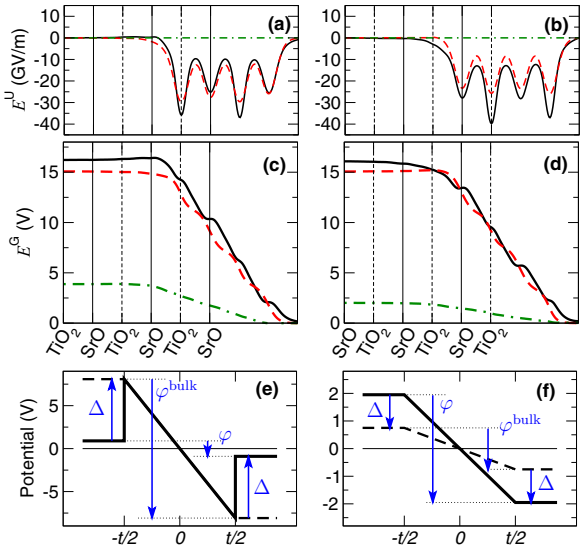

FIG. 2. (Color online) Electric field and potential response to mechanical deformations. The E_x^{U} [(a), (b)] and E_x^{G} [(c), (d)] response functions are shown for a SrO- [(a), (c)] and TiO_2-terminated [(b), (d)] slab. Solid black, dashed red, and dot-dashed green curves refer to longitudinal, transversal, and shear deformations, respectively. The location of the SrO (dashed) and TiO_2 (solid) atomic layers is indicated by vertical lines (only half of the symmetric slab is shown). Panels (e) and (f) show the electrostatic potential that would be induced in a macroscopic SrO-terminated slab of thickness t when subjected to a strain gradient of hypothetical magnitude $1/t$. The longitudinal (e) and shear (f) cases are shown, illustrating the qualitative difference in the response. Dashed and solid lines refer to the bulk and total contribution, respectively; $\Delta = \varphi^{\mathrm{surf}}/2$.

uniform deformation of the slab: the unperturbed $V(x)$ is a symmetric potential well, whose depth, ϕ, is modified by a diagonal strain component, $\varepsilon_{\beta\beta}$. Such a dependence of ϕ on the strain corresponds precisely to the surface contribution to the flexovoltage coefficient,

$$\varphi^{\mathrm{surf}}_{xx,\beta\beta} = \frac{d\phi}{d\varepsilon_{\beta\beta}} = -\int_0^{+\infty} dx\, E^{\mathrm{U}}_{x,\beta\beta}(x). \tag{7}$$

The functions $E^{\mathrm{G}}_{xx,\beta\beta}(x)$, describing the genuine strain-gradient effects, display a capacitor-like behavior: the field is uniform inside the film and zero outside, consistent with the open-circuit electrical boundary conditions (EBC) that were enforced. Interestingly, the uniform internal field, $E^{\mathrm{slab}}_{xx,\beta\beta} = E^{\mathrm{G}}_{xx,\beta\beta}(x=0)$, appears to be *independent* of the surface termination. This is not a coincidence: the open-circuit flexoelectric field in the longitudinal and transversal case is a bulk property of the material, and relates to the bulk flexovoltage coefficients [10,19] as

$$\varphi^{\mathrm{bulk}}_{xx,\beta\beta} = -E^{\mathrm{slab}}_{xx,\beta\beta}. \tag{8}$$

Thus, for a strain gradient of the type $\varepsilon_{\beta\beta,x}$, the analysis of the **E** response of the deformed slab yields complete information on both surface and bulk contributions to the flexoelectric effect [their respective impact on the electrostatic potential of a macroscopic film is illustrated in Fig. 2(e)]. Most importantly, we have thereby gained access to the transversal bulk flexovoltage coefficient, $\varphi^{\mathrm{bulk}}_{xx,yy}$, whose computation has eluded earlier first-principles attempts.

In the shear case, the flexoelectric field depends on both bulk and surface-specific properties [10], and is therefore termination-dependent [see Fig. 2(f)]; from the electric field response functions of Figs. 2(a)–2(d) we can thus only extract the *total* flexovoltage coefficient of the slab, $\varphi_{xy,xy} = -E^{\mathrm{slab}}_{xy,xy}$. To separate $\varphi_{xy,xy}$ into bulk and surface terms it suffices, however, to complement the above data with a calculation of bulk $SrTiO_3$. (Details are reported in the Supplemental Material [28], note 2.) The latter, in particular, yields two additional response quantities [16] describing the longitudinal components of φ^{bulk} along an arbitrary direction in space,

$$\varphi^{\mathrm{bulk}}_{\mathrm{L1}} = \varphi^{\mathrm{bulk}}_{xx,xx}, \tag{9}$$

$$\varphi^{\mathrm{bulk}}_{\mathrm{L2}} = \varphi^{\mathrm{bulk}}_{xx,yy} + 2\varphi^{\mathrm{bulk}}_{xy,xy}. \tag{10}$$

Equation (9) constitutes a useful consistency check of the methodology, as $\varphi^{\mathrm{bulk}}_{\mathrm{L1}}$ is redundant with the already calculated value of $\varphi^{\mathrm{bulk}}_{xx,xx}$. Equation (10), on the other hand, yields the sought-after value of $\varphi^{\mathrm{bulk}}_{xy,xy}$ since we already know $\varphi^{\mathrm{bulk}}_{xx,yy}$ from the slab calculations. Finally, we use $\varphi_{xy,xy} = -E^{\mathrm{slab}}_{xy,xy}$ to infer $\varphi^{\mathrm{surf}}_{xy,xy} = \varphi_{xy,xy} - \varphi^{\mathrm{bulk}}_{xy,xy}$.

Our results for the bulk, surface, and total flexovoltage coefficients of the truncated-bulk, frozen-ion deformation of a $SrTiO_3$ slab are summarized in Table I. At the bulk level, it is interesting to note the relatively small magnitude of the shear coefficients, $\varphi^{\mathrm{bulk}}_{xy,xy}$ and $\varphi^{\mathrm{surf}}_{xy,xy}$, compared to both the longitudinal and the transversal ones. Meanwhile, in the latter two cases there is a large cancellation between bulk and surface terms; as a result, the values of the total flexovoltage coefficients, φ, are all comparable in magnitude. This fact can be rationalized by observing that the linear response to atomic displacements, in a ionic (or partially ionic) solid, is largely dominated by the rigid displacement of an approximately spherical charge density distribution surrounding each atom. The spherical contribution, which is typically large and negative [9], shows up in $\varphi^{\mathrm{bulk}}_{xx,\beta\beta}$, and with opposite sign in $\varphi^{\mathrm{surf}}_{xx,\beta\beta}$; in the shear case neither the bulk nor the surface term is affected. (See Supplemental Material, note 1, of Ref. [10] and Fig. S2 therein.) Remarkably, the resulting values of φ depend

TABLE I. Frozen-ion flexovoltage coefficients of a truncated-bulk $SrTiO_3$ slab. To compute φ^{bulk} we used $\varphi^{\mathrm{bulk}}_{\mathrm{L1}} = -16.15$ V and $\varphi^{\mathrm{bulk}}_{\mathrm{L2}} = -18.07$ V (see Supplemental Material [28], note 2; the agreement with the values reported by Hong and Vanderbilt [16], $\varphi^{\mathrm{HV}}_{\mathrm{L1}} = -16.25$ V and $\varphi^{\mathrm{HV}}_{\mathrm{L2}} = -18.17$ V, is excellent), and $E^{\mathrm{slab}}_{xx,yy} = 15.08$ V [extracted from Figs. 2(c) and 2(d)]. (L), (T), and (S) stands for longitudinal, transversal, and shear, respectively. Volt units are used throughout.

	φ^{bulk}	φ^{surf}		φ (total)	
		SrO	TiO_2	SrO	TiO_2
xx,xx (L)	−16.15	14.36	16.95	−1.80	0.80
xx,yy (T)	−15.08	15.68	12.45	0.61	−2.63
xy,xy (S)	−1.50	−2.38	−0.51	−3.88	−2.01

TABLE II. Flexovoltage coefficients of a relaxed $SrTiO_3$ slab. The frozen-ion (FI), lattice-mediated (LM), and total relaxed-ion (RI = FI + LM) values of the bulk, surface, and total slab response are reported. Volt units are used throughout.

	φ^{bulk}	φ^{surf}		φ (total)	
		SrO	TiO_2	SrO	TiO_2
FI	−10.37	13.47	6.84	3.10	−3.53
LM	−0.44	−4.93	5.34	−5.38	4.90
RI	−10.81	8.53	12.18	**−2.28**	**1.37**

strongly on the details of the surface, and in some cases even have opposite signs in the SrO- and TiO_2-terminated slabs. Such a conclusion, in fact, persists after we take into account the full relaxation of the atomic structure; we shall prove this point in the following paragraphs.

To investigate the relaxed-ion response of the film, we shall consider an "effective" bending deformation of the type [10]

$$\varepsilon_{\text{eff},x} = \varepsilon_{yy,x} - \nu\varepsilon_{xx,x}. \tag{11}$$

The coefficient $\nu = \mathcal{C}_{xx,yy}/\mathcal{C}_{xx,yy}$ is the ratio of the transversal and longitudinal components of the bulk elastic tensor, $\mathcal{C}_{\alpha\beta\gamma\lambda}$, and accounts for the mechanical equilibrium condition; i.e., it ensures that the stress field vanishes everywhere in the interior of the deformed sample. (Our calculated value for $SrTiO_3$ is $\nu = 0.2914$.) As before, the overall flexovoltage coefficient of the slab can be written in terms of a bulk and a surface contribution,

$$\varphi_{xx,\text{eff}} = \varphi^{\text{bulk}}_{xx,\text{eff}} + \varphi^{\text{surf}}_{xx,\text{eff}}, \tag{12}$$

whose respective impact on the induced electrostatic potential follow the form of Fig. 2(e). The relaxed-ion (RI) value of $\varphi^{\text{bulk}}_{xx,\text{eff}}$ consists in a frozen-ion (FI) contribution, given by $\varphi^{\text{bulk,FI}}_{xx,\text{eff}} = \varphi^{\text{bulk}}_{xx,yy} - \nu\varphi^{\text{bulk}}_{xx,xx}$, plus a lattice-mediated (LM) part, which we calculate as detailed in the Supplemental Material [28], note 2. The corresponding contributions to $\varphi^{\text{surf}}_{xx,\text{eff}}$ are calculated by applying a uniform strain of the type $\varepsilon_{\text{eff}} = \varepsilon_{yy} - \nu\varepsilon_{xx}$ to fully relaxed slab supercells (see Supplemental Material [28], note 3).

A summary of the results is reported in Table II. The respective contributions of the bulk and surface are, overall, in line with the available order-of-magnitude estimates [22]. The values marked with boldface font, i.e., the flexovoltage coefficient of a fully relaxed $SrTiO_3$ slab subjected to bending, are the main result of this work. [The beam-bending case is easily recovered by multiplying the reported values by $\tau = \mathcal{C}_{xx,xx}/(\mathcal{C}_{xx,xx} + \mathcal{C}_{xx,yy})$. By using the calculated elastic constants of bulk $SrTiO_3$, reported in Table S2, we find $\tau = 0.77$.] Note their substantial departure with respect to the corresponding bulk coefficient, confirming the dramatic impact of the surface structural and electronic properties on the electromechanical response of the system. Remarkably, the aforementioned response coefficients are opposite in sign depending on whether a SrO- and TiO_2-terminated slab is considered. In fact, the surface shows an even larger termination dependence at the frozen-ion level, but with *opposite* sign: the LM contribution to φ^{surf} depends so strongly on the termination that its inclusion results in a voltage reversal, both in the TiO_2- and SrO-type slabs. (A microscopic analysis of the surface relaxations is provided in the Supplemental Material [28], note 3.) By contrast, the LM contribution to the bulk flexovoltage coefficient is relatively minor, about one order of magnitude smaller than any other value reported in the table, and of little impact on the final results. This constitutes a substantial departure from the commonly accepted idea that bulk lattice-mediated mechanisms are predominantly responsible for the flexoelectric polarization. On the contrary, our results indicate that by modifying the surface, one can fully control the magnitude, and even the sign, of the flexoelectric effect, in stark contrast with previous assumptions.

These results have profound implications, both for the interpretation of the experiments (where surface contributions are inevitably present) and for the optimization of electromechanical devices based on the flexoelectric effect. Regarding the experiments, the reported values [2] for the effective flexovoltage response of $SrTiO_3$ seem to cluster around 1–2 V, in fair agreement with our theoretical results; unfortunately, the available data are sparse and sometimes contradictory, which prevents a more detailed comparison. On the application side, our results demonstrate that surface/interface engineering may be a viable route towards controlling (and enhancing) the flexoelectric performance of a material such as $SrTiO_3$. Given the rich variety of surface structures and compositions that are accessible to perovskite oxides depending on thermodynamic conditions and treatment procedures, this opens up an essentially unlimited range of opportunities for device design.

This work was supported by MINECO-Spain (Grants No. MAT2010-18113, No. CSD2007-00041, and No. FIS2013-48668-C2-2-P) and by Generalitat de Catalunya (2014 SGR 301). We thankfully acknowledge the computer resources, technical expertise, and assistance provided by the Supercomputing Center of Galicia (CESGA).

[1] A. K. Tagantsev, Phys. Rev. B **34**, 5883 (1986).
[2] P. Zubko, G. Catalan, and A. K. Tagantsev, Annu. Rev. Mater. Res. **43**, 387 (2013).
[3] L. E. Cross, J. Mater. Sci. **41**, 53 (2006).
[4] G. Catalan, B. Noheda, J. McAneney, L. J. Sinnamon, and J. M. Gregg, Phys. Rev. B **72**, 020102 (2005).
[5] S.-I. Park, A.-P. Le, J. Wu, Y. Huang, X. Li, and J. A. Rogers, Adv. Mater. **22**, 3062 (2010).
[6] G. Catalan, A. Lubk, A. H. G. Vlooswijk, E. Snoeck, C. Magen, A. Janssens, G. Rispens, G. Rijnders, D. H. A. Blank, and B. Noheda, Nat. Mater. **10**, 963 (2011).
[7] H. Lu, C.-W. Bark, D. E. de los Ojos, J. Alcala, C. B. Eom, G. Catalan, and A. Gruverman, Science **336**, 59 (2012).
[8] A. K. Tagantsev and A. S. Yurkov, J. Appl. Phys. **112**, 044103 (2012).
[9] J. Hong and D. Vanderbilt, Phys. Rev. B **84**, 180101(R) (2011).
[10] M. Stengel, Nat. Commun. **4**, 2693 (2013).

[11] R. M. Martin, Phys. Rev. B **5**, 1607 (1972).
[12] L. C. Lew Yan Voon and M. Willatzen, J. Appl. Phys. **109**, 031101 (2011).
[13] M. Stengel and N. A. Spaldin, Nature (London) **443**, 679 (2006).
[14] M. Stengel, D. Vanderbilt, and N. A. Spaldin, Nat. Mater. **8**, 392 (2009).
[15] R. Resta, Phys. Rev. Lett. **105**, 127601 (2010).
[16] J. Hong and D. Vanderbilt, Phys. Rev. B **88**, 174107 (2013).
[17] R. Maranganti and P. Sharma, Phys. Rev. B **80**, 054109 (2009).
[18] J. Hong, G. Catalan, J. F. Scott, and E. Artacho, J. Phys.: Condens. Matter **22**, 112201 (2010).
[19] M. Stengel, Phys. Rev. B **88**, 174106 (2013).
[20] P. Zubko, G. Catalan, P. R. L. Welche, A. Buckley, and J. F. Scott, Phys. Rev. Lett. **99**, 167601 (2007).
[21] Strictly speaking φ^{surf} contains, in addition to genuine piezoelectric effects, also a metric contribution [10], which originates from the rigid deformation of the full charge density of the system. Such a contribution can be related to the so-called "surface flexoelectricity," as defined in Refs. [22,27].
[22] P. V. Yudin and A. K. Tagantsev, Nanotechnology **24**, 432001 (2013).
[23] X. Gonze, B. Amadon, P.-M. Anglade, J.-M. Beuken, F. Bottin, P. Boulanger, F. Bruneval, D. Caliste, R. Caracas, M. Côté *et al.*, Comput. Phys. Commun. **180**, 2582 (2009).
[24] X. Gonze, Phys. Rev. B **55**, 10337 (1997).
[25] A. Baldereschi, S. Baroni, and R. Resta, Phys. Rev. Lett. **61**, 734 (1988).
[26] J. Junquera, M. H. Cohen, and K. M. Rabe, J. Phys.: Condens. Matter **19**, 213203 (2007).
[27] A. K. Tagantsev, Phase Transitions **35**, 119 (1991).
[28] See Supplemental Material at http://link.aps.org/supplemental/10.1103/PhysRevB.90.201112 for a detailed description of the computational methods and extensive convergence tests.